Arch. Metall. Mater. **65** (2020), 2, 885-891

DOI: 10.24425/amm.2020.132835

M. POTOCZEK[1*], E. KOCYŁO[1], M. KRAUZ[2], A. TŁUCZEK[2]

ZrO_2 GELCAST FOAMS COATED WITH APATITE LAYERS

In this work, gel-casting of foams method was used to produce ZrO_2 porous ceramics. The obtained foams with total porosity of 89.5 vol% were composed of approximately spherical cells having the mean diameter of 537 ± 153 μm interconnected by circular cell windows having the mean diameter of 152 ± 82 μm. Next, the ZrO_2 foams were coated with fluorapatite (FA) and hydroxyapatite (HA) layers by slurry infiltration. The intermediate fluorapatite (FA) layer was introduced to prevent the chemical reactions between ZrO_2 and HA at high temperatures during sintering process. The ZrO_2 samples containing only HA coatings, were also tested, for comparison. The obtained ceramic biomaterials were subjected to in vitro tests in the simulated body fluid (SBF) solution. The results show that the ZrO_2 foams with FA/HA layers possessed better bioactivity than the foams with the HA/HA coating.

Keywords: gel-casting of foams, porous ZrO_2, fluorapatite (FA), hydroxyapatite (HA) coating

1. Introduction

Recent developments in bioceramics research are focused on bioactive ceramics, such as hydroxyapatite [HA, $Ca_{10}(PO_4)_6(OH)_2$], as it exhibits superior biological properties over other materials. It is one of a few bioactive materials capable of creating a direct and firm bond with the bone tissue, due to the similarity of its chemical composition and crystallography to those of mineralized bone of human tissues [1]. However, HA shows poor mechanical properties and hence applications of HA to bioceramics are limited to powders, granules and non-load bearing parts [2]. The ceramic material which shows excellent mechanical properties is zirconium dioxide (ZrO_2). ZrO_2 also shows biocompatibility, and good chemical stability, and it has been used in many biomedical applications as an inert biomaterial [3].

In most applications of biomedical materials the high mechanical properties as well as the chemical reactivity of their surfaces are especially important. For this reason, it is highly desirable to combine the mechanical properties of zirconia with the bioactivity of hydroxyapatite, for example through the application of the HA coating systems onto ZrO_2. However, there is a problem in these composites because HA and ZrO_2 react in high temperatures to form α- or β-tricalcium phosphate (TCP, $Ca_3(PO_4)_2$) and calcium zirconate ($CaZrO_3$), as follows (1):

$$Ca_{10}(PO_4)_6(OH)_2 + ZrO_2 \rightarrow 3Ca_3(PO_4)_2 + CaZrO_3 + H_2O \quad (1)$$

The decomposition process of HA in the presence of ZrO_2 degrades the mechanical properties and the biocompatibility of the material [4]. Therefore, it is necessary to suppress the reaction between HA and ZrO_2. Fluorapatite [FA, $Ca_{10}(PO_4)_6F_2$] was shown in the literature as a material that fulfil these requirements, as it is introduced as an intermediate layer between ZrO_2 and HA [5-6]. The excellent chemical stability of fluorapatite with respect to ZrO_2 has effectively prevented the reaction (1). Moreover, FA exhibits good biocompatibility, lower solubility, much higher thermal and chemical stability with respect to HA [7].

Several researchers have successfully fabricated a porous ZrO_2 body as a framework for load-bearing with HA as an outer coating layer and FA as an intermediate layer [5-6]. In the above studies, apatite coatings were applied to porous ZrO_2 produced by the replication of a polyurethane foam template method. The replication of a polyurethane foam template method is one of the most common methods for fabrication of porous ceramics. The major problem of the sponge replication technique is low mechanical strength, due to the presence of large number of cracks in the hollow struts, that arise as a result of the volatilization of the organic filament used as a substrate [8]. On the other hand, direct foaming followed by consolidation of the wet

[1] RZESZÓW UNIVERSITY OF TECHNOLOGY, FACULTY OF CHEMISTRY, 6 POWSTAŃCÓW WARSZAWY STR., 35-959 RZESZÓW, POLAND
[2] INSTITUTE OF POWER ENGINEERING, CERAMIC DEPARTMENT CEREL, 1 TECHNICZNA STR., 36-040 BOGUCHWAŁA, POLAND
* Corresponding author: potoczek@prz.edu.pl

foam by gel-casting leads to higher strength than replica foams at the same porosity level due to the presence of well-densified struts. Gel-casting of porous materials was developed as a result of the combination of the gel-casting process and the aeration of ceramic suspensions [9-10]. Wet foams stabilized by surfactants require a gelling agent to consolidate the foam microstructure before extensive coalescence and disproportionation take place. The next step is calcinations of organic additives followed by sintering at high temperature. The obtained ceramic foams consist of interconnected porous network of spherical cells interconnected by circular cell windows [11]. Due to the relatively high mechanical strength and open porosity gel-cast foams have many application fields as highly-porous biomaterials as well as other ceramics such as filters, catalyst supports, matrixes for ceramic-metal or ceramic-polymer composites, etc. [11-18].

However, in literature there are no data on gel-cast ZrO_2 foams coated with apatite layers. Therefore, the present study aims to fabricate of porous ZrO_2 by the gel-casting of foams method followed by coating with FA and subsequently with HA using the slurry infiltration technique. The obtained ceramic biomaterials were characterized in terms of their phase composition and morphology as well as their bioactivity.

2. Materials and methods

2.1. Preparation of ZrO_2 foams

A commercial yttria-stabilized zirconia powder (TZ-3YS-E, Tosoh, Japan, granules size d_{50} = 0.6 μm) was used as the ceramic powder.

Ceramic suspension with a high amount of ZrO_2 powder as a solid phase (36.9 vol%) was prepared by adding 1.5 wt% of dispersant (Dolapix PC75, Zschimmer & Schwarz, Germany) as was suggested by Adolfsson [19] for successfully dispersing zirconia (TZ-3YS-E) water suspensions. Homogenization was carried out in a planetary ball mill (PM 100 Retsch, Germany) at 250 rpm for 1 h.

Agarose (Erbamea, Italy; impurities: water content ≤7%, ash ≤0.5%, sulphate ≤0.14%) was selected as a gelling agent. Solution with a concentration of 4 wt% of agarose was prepared in a water bath at 95°C for 1 h in order to avoid occurrence of undissolved agarose in the ceramic suspension. Then the agarose solution was cooled down to 65°C and added to the zirconia suspension which was in the meantime warmed at the same temperature. The final ZrO_2 content in ceramic suspension was fixed at 32.8 vol%. The total concentration of active gelling matter was fixed at 0.66 wt% with regard to water which corresponded to 0.22 wt% with regard to zirconia powder.

The rheological behavior of the suspension with varied agarose contents was conducted at 60°C with a rotary rheometer (KinexusPro, Malvern) fitted with double concentric cylinder geometry. The tests were carried out in the shear rate range from 0.1 s^{-1} to 1000 s^{-1}.

Foaming was conducted through agitation, with the help of a double-blade mixer at 65°C. Addition of nonionic surfactants (Tergitol TMN-10, Sigma-Aldrich, Germany and Simulsol SL-26, Seppic, France) was necessary to stabilize the foam. The amount of Tergitol and Simulsol in 100 ml of the slurry were 0.4 ml and 1.6 ml, respectively. The foamed suspension containing agarose was poured into a mould. Gelation was performed by cooling the foam to 15°C, using flowing cold water. The green body was then de-moulded and left in room conditions during a few days to dry. Sintering was performed at 1450°C with 2 h dwell time using heating rate of 1.5°C/min to 700°C and then 4°C/min up to sintering temperature.

2.2. Characterization of ZrO_2 foams

The helium density of finely ground ZrO_2 foams was determined by helium pycnometer (Accu Pyc 1340). The apparent density, and open porosity of the ZrO_2 foams were measured by the water-immersion technique using the Archimedes method. Total porosity was evaluated based on the helium and the apparent densities according to Eq. (2):

$$P = \frac{\rho_s - \rho_a}{\rho_s} \cdot 100\% \quad (2)$$

where: P is total porosity of the foam (vol%); ρ_s and ρ_a are the helium density (g/cm^3) and the apparent density (g/cm^3), respectively.

The microstructure of the ZrO_2 foams was observed on scanning electron microscopes (Jeol JSM-5500 LV and Zeiss Ultra Plus). SEM pictures for monitoring cellular microstructure of the sintered bodies were analyzed in terms of estimation of cell sizes (spherical pores) and window sizes (interconnected pores). The diameter of minimum 150 cells and 350 cell windows were measured for each sample.

Pore size distribution (0.005-360 μm) of the ZrO_2 samples were evaluated by mercury intrusion porosimetry (AutoPore IV 9500, Micromeritics).

The compressive strength was measured by uniaxial compression (5982 UTM, Instron, Norwood, MA, USA). Test specimens with a nominal size of 10 mm × 10 mm × 15 mm were cut from larger pieces of the foam. The crosshead speed was 1.5 mm/min. In all mechanical determinations results were based on average of five samples.

2.3. Preparation of HA, FA slurries and coating process

The initial powders for each coating slurry were prepared from HA (Merck, Germany), and FA. The FA powder was fabricated from a reaction between tricalcium phosphate (Merck, Germany) and CaF_2 (Alfa Aesar, Germany) at 1000°C for 3 h in air [4]. Each powders were mixed with TEP (triethyl phosphate, Merck, Germany) and PVB (polyvinyl butyral, Sigma-Aldrich,

USA) in ethanol (Chempur, Poland) and stirred for 24 h to prepare the HA and the FA slurry. Loading of HA and FA powders were fixed at 30 wt% relative to ethanol. TEP and PVB were used as a dispersant and a binder, respectively, and the amounts were 5 wt% with respect to powder.

The zirconia-apatite composites were prepared by slurry infiltration technique in a vacuum oven (Nüve EV018) using a vacuum pump (Ilmvac GmbH, Germany), under reduced pressure ($1 \cdot 10^3$ Pa) for 2 min.

To fabricate an FA/HA double coating layer on ZrO_2, the FA layer was coated first, and then HA was coated on the sintered FA layer. The ZrO_2 samples were immersed into the FA slurry and then dried at room temperature and subsequently at 80°C for 3 h. Coated samples were heat treated at 800°C for 5 h and further at 1200°C for 1 h. The FA-coated body was immersed in the HA slurry, dried and heat treated following the same procedures. For a comparison, HA was coated twice onto the ZrO_2 body without the FA layer.

2.4. Characterization of ZrO_2 – apatite samples

The specific surface area of the coated ZrO_2 samples was determined by BET method (Micromeritics 3 Flex). The morphology of the coated ZrO_2 samples, before and after immersion in SBF, were examined by scanning electron microscopy (SEM, Zeiss Ultra Plus).

The phase composition of the coated ZrO_2 after heat treatment at 1200°C was investigated by X-ray diffraction (XRD, Bruker AXS D8 Advance, Karlsruhe, Germany).

The in vitro bioactivity assessments of zirconia-apatite samples were carried out by their immersion in simulated body fluid (SBF) solution for 28 days at 36.5°C. The SBF solution were prepared according to the formula described by Kokubo [20], with the concentration of ions nearly equal to those of the human blood plasma (Table 1). The samples (12.5 mm × 8 mm × 8 mm) were immersed in SBF and placed in an incubator (Incubator IC240, SalvisLab Incucenter, Rotkreuz, Switzerland) at 36.5°C for 28 days. The ion exchange between the SBF and sample was recorded using a conductivity meter CPC-551 (Elmetron, Zabrze, Poland) for different time periods. At the end of the period, the samples were removed from SBF, gently washed with deionized water and left to dry in an incubator that maintained a temperature of 36.5°C. The mass gain of the samples was determined by weighting them before and after the immersion test in SBF.

3. Results and discussion

3.1. Rheology of ZrO_2 suspensions

Fig. 1 shows the influence of agarose (wt% on a dry solid basis) on the viscosity of 32.8 vol% zirconium dioxide suspensions at 60°C. Even a small addition of agarose (0.22 wt% with regard to ZrO_2 powder) increased the viscosity of the suspension at the shear rates used in the present study. This effect was expected, since the agarose solution has generally higher viscosity than pure water. As can be seen from Fig. 1, the ZrO_2 slurries were pseudoplastic in behavior which is typical for concentrated ceramic suspensions. The effect of agarose concentration on the rheological properties of ZrO_2 suspensions was characterized by the n and k parameters (Table 2) calculated according to the Ostwald-de Waele relationship (Eq. (3)) [21].

$$\eta = k\gamma^{n-1} \tag{3}$$

where: η is a suspension viscosity (Pa·s), γ is a shear rate (s^{-1}), n is the power-law index of the fluid, and k is a consistency factor. As the agarose concentration increased, the value of the n index decreased which meant a shift towards a non-Newtonian fluid.

TABLE 1

Nominal ion concentrations of SBF in comparison with those in human blood plasma [20]

	Ion concentrations (mM)								
	Na^+	K^+	Mg^{2+}	Ca^{2+}	Cl^-	HCO_3^-	HPO_4^{2-}	SO_4^{2-}	pH
SBF	142.0	5.0	1.5	2.5	147.8	4.2	1.0	0.5	7.2-7.4
Blood plasma	142.0	5.0	1.5	2.5	103.0	27.0	1.0	0.5	7.40

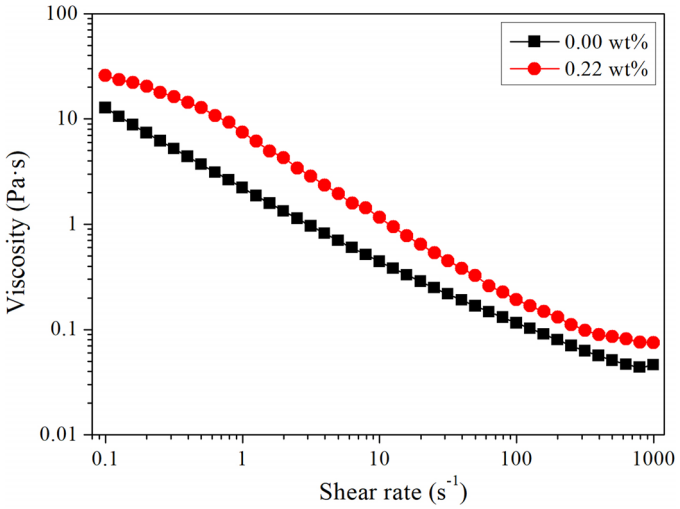

Fig. 1. The viscosity of zirconia suspensions at 60°C with the fixed solids loading of 32.8 vol% and various agarose contents

TABLE 2

The n and k parameters as a function of agarose concentration

Agarose concentration (wt% with regard to zirconia powder)	n (-)	k (Pa·s^2)
0.00	0.41	0.23
0.22	0.25	0.80

On the other hand, the calculated *k* parameter which is a consistency factor, increases with increasing agarose concentration in the ceramic suspension.

3.2. Physical and mechanical properties of the ZrO_2 foam

The helium and apparent densities of the ZrO_2 foam were 5.92 and 0.63 g/cm^3, respectively. The open porosity was measured as 88.9 ± 0.5 vol%. The calculated total porosity of the ZrO_2 foam was 89.5 ± 0.2 vol%. The compression strength of the 89.5 vol% ZrO_2 foam was measured as 1.8 ± 0.4 MPa.

3.3. Microstructure and pore size distribution of the ZrO_2 foam

The morphology of the sintered foams having 89.5 vol% total porosity is presented in Fig. 2. The SEM results reveal that ZrO_2 foams were typically composed of large spherical cells, interconnected by circular cell windows (Fig. 2a). Spherical pores were associated with densified polycrystalline struts (Fig. 2b). The image analysis of SEM micrographs showed that the foams had a mean cell size and a mean cell window size of 537 ± 153 μm and 152 ± 82 μm, respectively. The mode of the cell diameters was 440 μm, while the mode of the cell windows diameter was 93 μm.

The cell windows size obtained by SEM was complemented with the porosimetry data analyses. The peak of mercury intrusion porosimetry curve presented in Fig. 3 is sharp which indicates a narrow pore size distribution (20 to 350 μm), with the mode diameter of 141 μm. Data obtained by mercury porosimetry differ from those obtained by image analysis. The cell contains from a few to several windows of different diameters (Fig. 2a), hence mercury penetrates inside the cells through the windows of the largest diameter. The image analysis method specifies all cell window sizes. Therefore, the window cell size values obtained by mercury porosimetry are greater than those determined by image analysis.

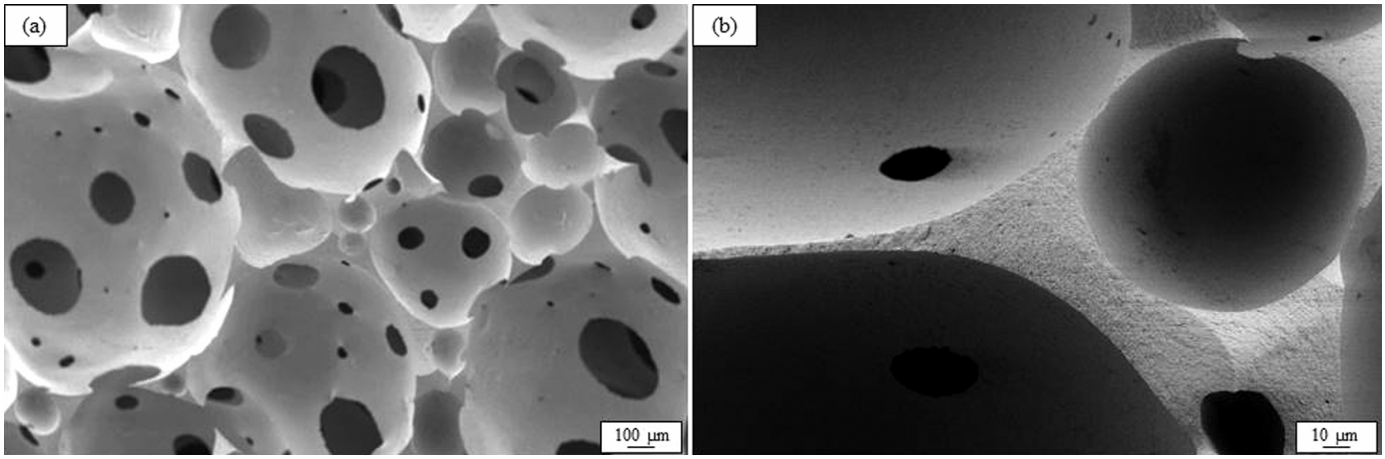

Fig. 2. SEM images of the ZrO_2 foams having total porosity of 89.5 vol% (a) surface morphology, (b) cross-sectional view of the strut

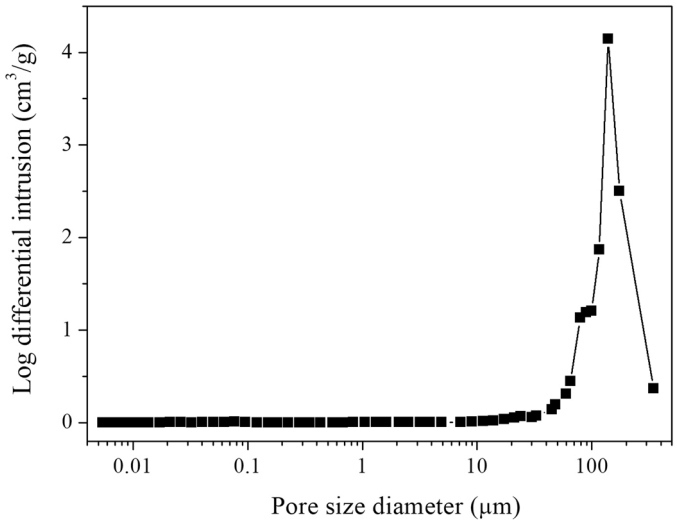

Fig. 3. Pore size distribution of the ZrO_2 foam determined by mercury intrusion porosimetry

3.4. Phase composition and morphology of apatite coating layer

Fig. 4(a-b) shows the X-ray diffraction patterns of the ZrO_2 after coating with HA double layer (HA/HA) and HA with FA intermediate layer (FA/HA) after final heat treatment at 1200°C for 1 h. The FA intermediate layer prevented the reaction between HA and ZrO_2 at 1200°C and suppressed the decomposition of HA. When HA was coated directly on ZrO_2 the heat treatment resulted in the decomposition of HA, with β-TCP being produced as shown in Fig. 4a. When the FA layer was present between HA and ZrO_2, the decomposition of HA was effectively suppressed, as manifested by Fig. 4b. No other peaks except for characteristic zirconia and apatite peaks were observed in the ZrO_2/FA/HA sample. Further increases in temperature up to 1300°C results accessory decomposition of HA with the formation of $CaZrO_3$ and α-TCP, according to Eq. (1), as was shown by other researches [22].

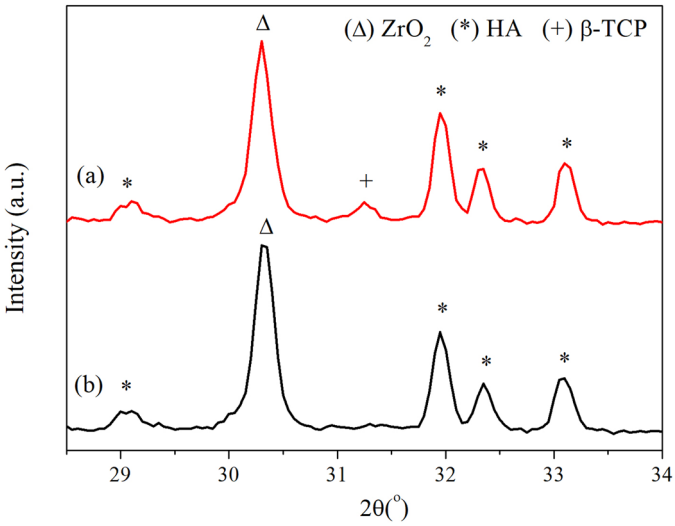

Fig. 4. X-ray diffraction patterns of ZrO_2 coated with: (a) HA double layer (HA/HA) and (b) HA with FA intermediate layer (FA/HA) after final heat treatment at 1200°C for 1 h: (Δ) ZrO_2, (*) HA, (+) β-TCP

SEM morphologies of the apatite coating layer on ZrO_2 are shown in Fig. 5. The microstructure maintained the initial structure without significant clogging of the pores, as was shown in Fig. 5a. The cross-sectional view showed the HA coating layer onto the FA pre-coated ZrO_2 samples (Fig. 5b). The FA/HA coating was bonded quite tightly and no cracks or delamination were observed at the interface or within the layers.

The obtained BET values of the specific surface area for ZrO_2/FA/HA and ZrO_2/HA/HA samples were 0.311 ± 0.002 and 0.312 ± 0.001 m^2/g, respectively.

3.5. Bioactivity in simulated body fluid (SBF)

The bioactivity of ZrO_2/FA/HA ceramics has been confirmed by the measurements of the mass change of samples subjected to immersion in SBF. After 28 days of incubation, the weight gain of ZrO_2/FA/HA was 2.311 ± 0.101 wt%, while for ZrO_2/HA/HA and ZrO_2 materials it was lower and amounted to 1.795 ± 0.044 wt% and 0.193 ± 0.027 wt%, respectively. Fig. 6 shows the surface morphology of the specimens after immersion in SBF solution for 28 days. On the surface of all samples, the formation of a precipitate is visible. After immersion in SBF, a large number of precipitates were noticed on the ZrO_2/FA/HA surface (Fig. 6a), much smaller amount on the ZrO_2/HA/HA surface (Fig. 6b), whereas only a very small number of precipitates were formed on the ZrO_2 surface (Fig. 6c). This shows that among the tested materials, the specimen containing FA has the best bioactivity.

Fig. 7 shows a change in ionic conductivity during incubation of the samples in simulated body fluid (SBF) solution for 28 days at 36.5°C. The ionic conductivity of the SBF solution containing a pure ZrO_2 foam remained almost constant throughout the soaking period. The ionic conductivity of the SBF solution containing the ZrO_2 foam coated by HA layers but without an intermediate FA layer (ZrO_2/HA/HA) decreases significantly during the first week of incubation and stays almost constant after that. Therefore, the growth of the apatite layer takes place which consumes calcium and phosphate ions in SBF causing the ionic conductivity decrease [23]. For (ZrO_2/FA/HA) samples, changes in ionic conductivity were similar, however, the presence of FA in composites influenced the in vitro behavior. A greater decrease in ionic conductivity for samples containing FA indicates a faster formation of apatite on their surface. The data in Fig. 7 show that fluorapatite outperforms hydroxyapatite coatings in terms of bioactivity which is consistent with the morphological observations (Fig. 6). It should be noted, that in the case of porous materials bioactivity is dependent on specific surface area. Our BET results showed that the specific surface area for ZrO_2/HA/HA/ and ZrO_2/FA/HA composites were almost the same (see previous section). Therefore, our studies clearly indicated the intermediate FA layer effect on the composite bioactivity in SBF solution.

4. Conclusions

In this work, the gel-casting of foams method was used to produce ZrO_2 porous ceramics. The effect of agarose concentration on the rheological properties of ZrO_2 suspensions

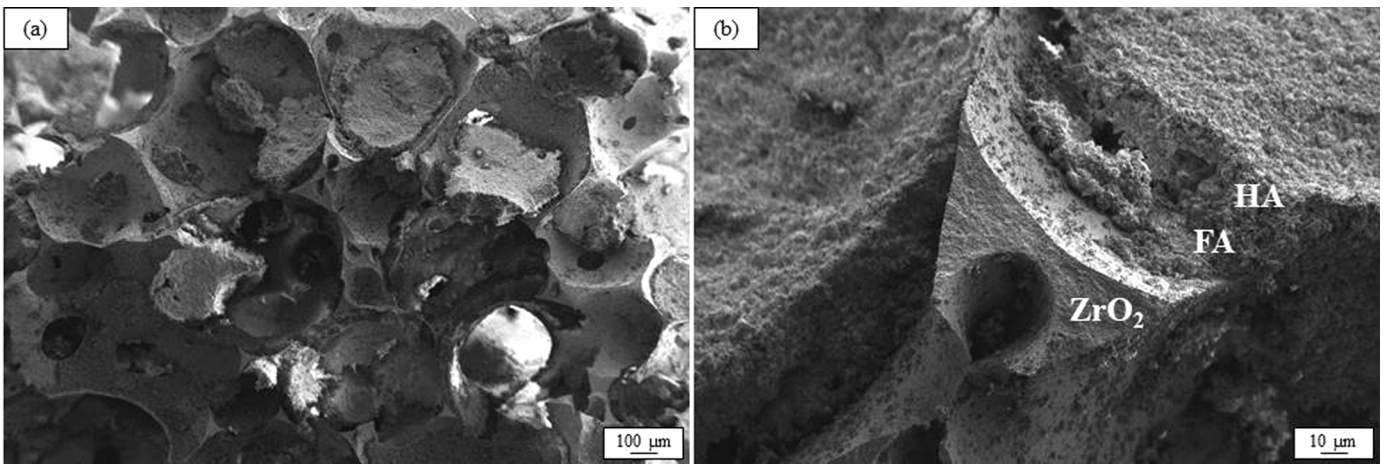

Fig. 5. Morphology of an apatite layer on the ZrO_2 substrate: (a) surface morphology, (b) cross-section view with high magnification

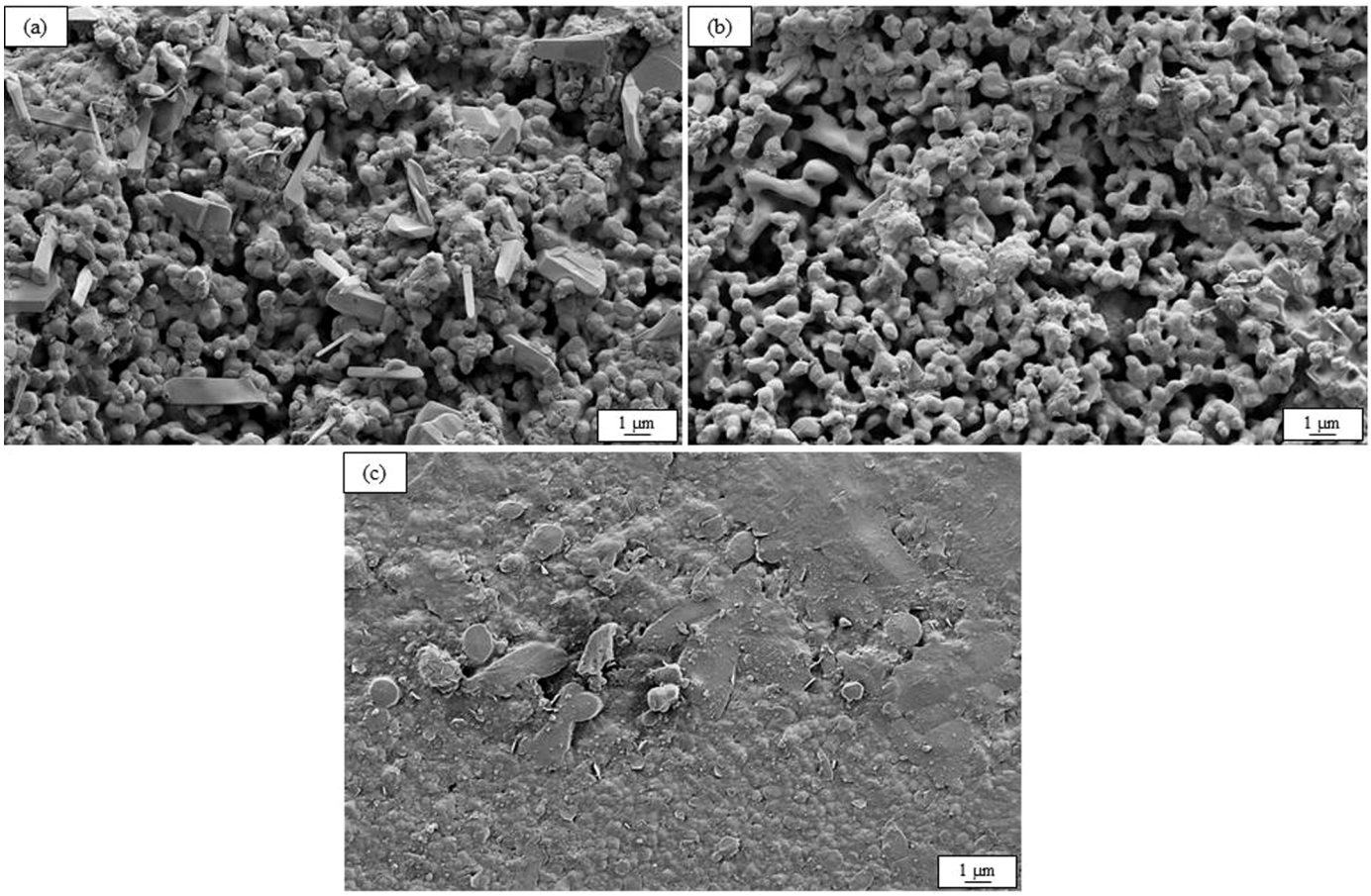

Fig. 6. Surface morphologies of: (a) ZrO_2/FA/HA, (b) ZrO_2/HA/HA and (c) ZrO_2 after soaking in SBF solution for 28 days

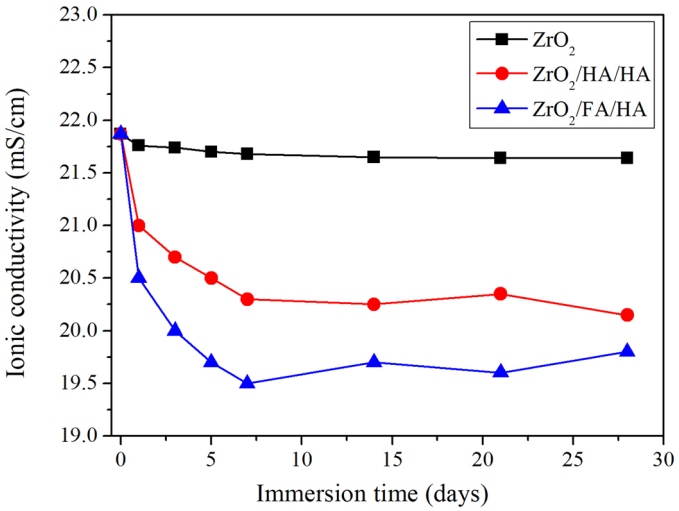

Fig. 7. Ionic conductivity vs. immersion time in SBF solution containing: ZrO_2/FA/HA, ZrO_2/HA/HA and ZrO_2 porous samples

was explained. The obtained ZrO_2 foams with total porosity of 89.5 vol% were composed of approximately spherical cells (537 ± 153 μm) interconnected by circular cell windows (152 ± 82 μm). Next, the ZrO_2 gel-cast foams were coated with bioactive ceramic layers by slurry infiltration method. In order to suppress the reaction between hydroxyapatite and ZrO_2 occurring during sintering, fluorapatite as an intermediate layer was introduced. Bioactivity of the obtained ceramic biomaterials was evaluated by their immersion in the simulated body fluid (SBF) solution. The studies indicated that the ZrO_2 foams coated by FA and HA layers showed better bioactivity, than those coated by HA layers without an intermediate FA layer.

Acknowledgements

Financial support from Rzeszów University of Technology (DS.CM.19.001) is gratefully acknowledged.

REFERENCES

[1] A. Rapacz-Kmita, A. Ślósarczyk, Z. Paszkiewicz, J. Eur. Ceram. Soc. **26** (8), 1481-1488 (2006), DOI: 10.1016/j.jeurceramsoc.2005.01.059.

[2] Y. Nayak, R. Rana, S. Pratihar, S. Bhattacharyya, Int. J. Appl. Ceram. Technol. **5** (1), 29-36 (2008), DOI: 10.1111/j.1744-7402.2008.02180.x.

[3] C. Piconi, G. Maccauro, Biomaterials **20**, 1-25 (1999), DOI: 10.1016/s0142-9612(98)00010-6.

[4] H.-W. Kim, Y.-M. Kong, Y.-H. Koh, H.-E. Kim, H.-M. Kim, J.S. Ko, J. Am. Ceram. Soc. **86** (12), 2019-2026 (2003), DOI: 10.1111/j.1151-2916.2003.tb03602.x.

[5] H.-W. Kim, H.-E. Kim, V. Salih, J.C. Knowles, J. Biomed. Mater. Res. A **68** (3), 522-530 (2004), DOI: 10.1002/jbm.a.20094.

[6] H.-W. Kim, S.-Y. Leea, C.-J. Baea, Y.-J. Noha, H.-E. Kim, H.-M. Kim, J.S. Ko J, Biomaterials **24** (19), 3277-3284 (2003), DOI: 10.1016/S0142-9612(03)00162-5.

[7] A. Bianco, I. Cacciotti, M. Lombardi, L. Montanaro, E. Bemporad, M. Sebastiani, Ceram. Int. **36** (1), 313-322 (2010), DOI: 10.1016/j.ceramint.2009.09.007.

[8] P. Sepulveda, F.S. Ortega, M.D.M. Innocentini, V.C. Pandolfelli, J. Am. Ceram. Soc. **83** (12), 3021-3024 (2000), DOI: 10.1111/j.1151-2916.2000.tb01677.x.

[9] P. Sepulveda, J.G.P. Binner, J. Eur. Ceram. Soc. **19** (12), 2059-2066 (1999), DOI: 10.1016/S0955-2219(99)00024-2.

[10] M.D.M. Innocentini, P. Sepulveda, V.R. Salvini, V.C. Pandolfelli, J. Am. Ceram. Soc. **81** (12), 3349-3352 (1998), DOI: 10.1111/j.1151-2916.1998.tb02782.x.

[11] M. Potoczek, R.E. Śliwa, Arch. Metall. Mater. **56** (4), 1265-1269 (2011), DOI: 0.2478/v10172-011-0145-2.

[12] M. Potoczek, A. Zima, Z. Paszkiewicz, A. Ślósarczyk, Ceram. Int. **35** (6), 2249-2254 (2009), DOI: 10.1016/j.ceramint.2008.12.006.

[13] H. Ghomi, M.H. Fathi, H. Edris, Mater. Res. Bull. **47** (11), 3523-3532 (2012), DOI: 10.1016/j.materresbull.2012.06.066.

[14] M.D.M. Innocentini, R.K. Faleiros, R. Pisani, Jr., I. Thijs, J. Luyten, S. Mullens, J. Porous Mater. **17** (5), 615-627 (2010), DOI: 10.1007/s10934-009-9331-2.

[15] I. Santacruz, R. Moreno, J.B. Rodrigues Neto, Int. J Appl. Ceram. Technol. **5** (1), 74-83 (2008), DOI: 10.1111/j.1744-7402.2008.02189.x.

[16] J. Ligoda-Chmiel, M. Potoczek, R.E. Śliwa, Arch. Metall. Mater. **60** (4), 2757-2762 (2015), DOI: 10.1515/amm-2015-0444.

[17] J. Ligoda-Chmiel, R.E. Śliwa, M. Potoczek, Compos. Part B Eng. **112**, 196-202 (2017), DOI: 10.1016/j.compositesb.2016.12.041.

[18] M. Potoczek, A. Chmielarz, M.D.M. Innocentini, I.C.P. da Silva, P. Colombo, B. Winiarska, J. Am. Ceram. Soc. **101** (12), 5346-5357 (2018), DOI: 10.1111/jace.15802.

[19] E. Adolfsson, J. Am. Ceram. Soc. **89** (6), 1897-1902 (2006), DOI: 10.1111/j.1551-2916.2006.01040.x.

[20] T. Kokubo, H. Takadama, Biomaterials **27**, 2907-2915 (2006), DOI: 10.1016/j.biomaterials.2006.01.017.

[21] K. Vajravelu, K.V. Prasad, P.S. Datti, B.T. Raju, Ain Shams Eng. J. **5**, 157-167 (2014), DOI: 10.1016/j.asej.2013.07.009.

[22] H.-W. Kim, B.-H. Yoon, Y.-H. Koh, H.-E. Kim, J. Am. Ceram. Soc. **89** (8), 2466-2472 (2006), DOI: 10.1111/j.1551-2916.2006.01114.x.

[23] N.S. Sambudi, S. Cho, K. Cho, RSC Adv. **6** (6), 43041-43048 (2016), DOI: 10.1039/C6RA03147A.